ce/papers The online collection for conference papers in civil engineering
Ernst & Sohn A Wiley Brand

EUROSTEEL 2017, September 13–15, 2017, Copenhagen, Denmark

Cyclic backbone curves for steel wide-flange columns: A numerical study

Gulen Ozkula*,[a], John Harris[b], Chia-Ming Uang[a]

[a]University of California, San Diego, Dept. Structural Engineering, U.S.A.
gozkula@ucsd.edu, cmu@ucsd.edu

[b] National Institute of Standards and Technology, U.S.A.
john.harris@nist.gov

ABSTRACT

Experimental and analytical studies on the cyclic behaviour of deep, slender wide-flange steel beam-columns funded by the National Institute of Standards and Technology (NIST) is ongoing at the University of California at San Diego (UCSD). In parallel with full-scale column tests, numerical simulations of columns under monotonic and cyclic loading conditions were conducted to generate a wide-ranging database of results. A correlation study using results from the full-scale tests was conducted to validate the numerical simulation procedure. The simulated columns covered a wide range of cross-sectional (local) and member (global) slenderness ratios, axial force level, and yield stress. Regression analyses were conducted to construct moment-rotation responses, 'backbone curves', for use in performance-based evaluations of steel moment frames. The database is divided into three groups based on observed buckling modes. Computational expressions for the key parameters that define the backbone curves are presented.

Keywords: steel beam-column, cyclic behaviour, backbone curve, plastic rotation, buckling, slenderness ratios

1 INTRODUCTION

Prior to the 1994 Northridge earthquake, it was common practice to use shallow wide-flange sections (e.g., W310 [W12] or W360 [W14]) for steel moment frame construction because of their small footprint; thereby maximizing architectural flexibility in floor layouts. After the earthquake, a significant amount of research was conducted in the U.S. to address observed brittle fractures in the beam-to-column moment connections; some of the findings are reflected in AISC 341 [1]. This research also resulted in AISC 358 [2] which prescribes several prequalified moment connections that can be used for seismic-resistant moment frame construction.

Since the Northridge earthquake, engineers in the U.S. have turned to using deeper, slenderer steel columns to achieve an economic design that satisfies code-enforced story drift requirements [3]. However, since the slenderness ratios for local buckling and global buckling are significantly higher with deep columns, these columns are prone to various forms of buckling that impair their gravity load-carrying capacity [4, 5]. Past research on the cyclic behaviour of W360 [W14] columns (nominal depth = 356 mm [14 in.]) under axial compression and cyclic drift for braced frame applications in high seismic regions was conducted by Newell and Uang [6]. Unfortunately, little research is available to support the seismic design or assessment provisions of deep columns in moment frame applications prescribed in AISC 341 [1] and ASCE 41 [7]. To fill this gap, NIST developed a comprehensive research plan to study the seismic behaviour and design of deep, slender wide-flange steel beam-columns [8]. Experimental tests of twenty-five deeper (W610 [W24]) columns with a nominal depth of 610 mm [24 in.] were conducted recently at UCSD [5]; ASTM A992 steel with a specified minimum yield stress of 345 MPa [50 ksi] was used. Three levels of axial compression were considered: C_a = 0.2, 0.4, and 0.6, where C_a is the axial force ratio (= P / ϕ P_y with ϕ = 0.9 and P_y = nominal axial yield strength). Defining λ_f as the slenderness parameter for flange local buckling (FLB) (= b_f / 2t_f, where b_f = flange width and t_f = flange thickness), λ_w as the slenderness parameter

for web local buckling (WLB) (= h / t_w, where h = web depth and t_w = web thickness), and λ_L as the slenderness parameter for lateral-torsional buckling (LTB) (= L / r_y, where L = member length for the test specimens (= 5500 mm [18 ft.]) and r_y = radius of gyration about weak-axis (y-axis)), the tested column specimens covered the following slenderness ranges:

$$4.81 \leq \lambda_f \leq 6.94; \quad 28.7 \leq \lambda_w \leq 54.6; \quad 71.1 \leq \lambda_L \leq 161.2 \tag{1}$$

Prior to the NIST-funded deep column program, AISC sponsored a project to evaluate the cyclic behaviour of shallow columns commonly classified as stocky [7]. Nine W360 [W14] columns with the following slenderness parameters were tested:

$$3.1 \leq \lambda_f \leq 7.14; \quad 6.9 \leq \lambda_w \leq 17.7; \quad 42.2 \leq \lambda_L \leq 47.9 \tag{2}$$

The slenderness ratios for WLB and LTB of these stocky sections are significantly lower than those of the columns used in the NIST project. Based on the test results from the AISC and NIST projects, it was observed that the cyclic response of a steel column is highly dependent on the governing buckling mode developed during or after the formation of plastic hinges at the ends of the column. This buckling mode is a function of the cross-sectional (local) and member (global) slenderness ratios of the column. Even under high axial load levels, stocky W360 [W14] column could reach a high story drift (0.07 to 0.09 radians) with minor strength degradation and local buckling [Fig. 1(a)].

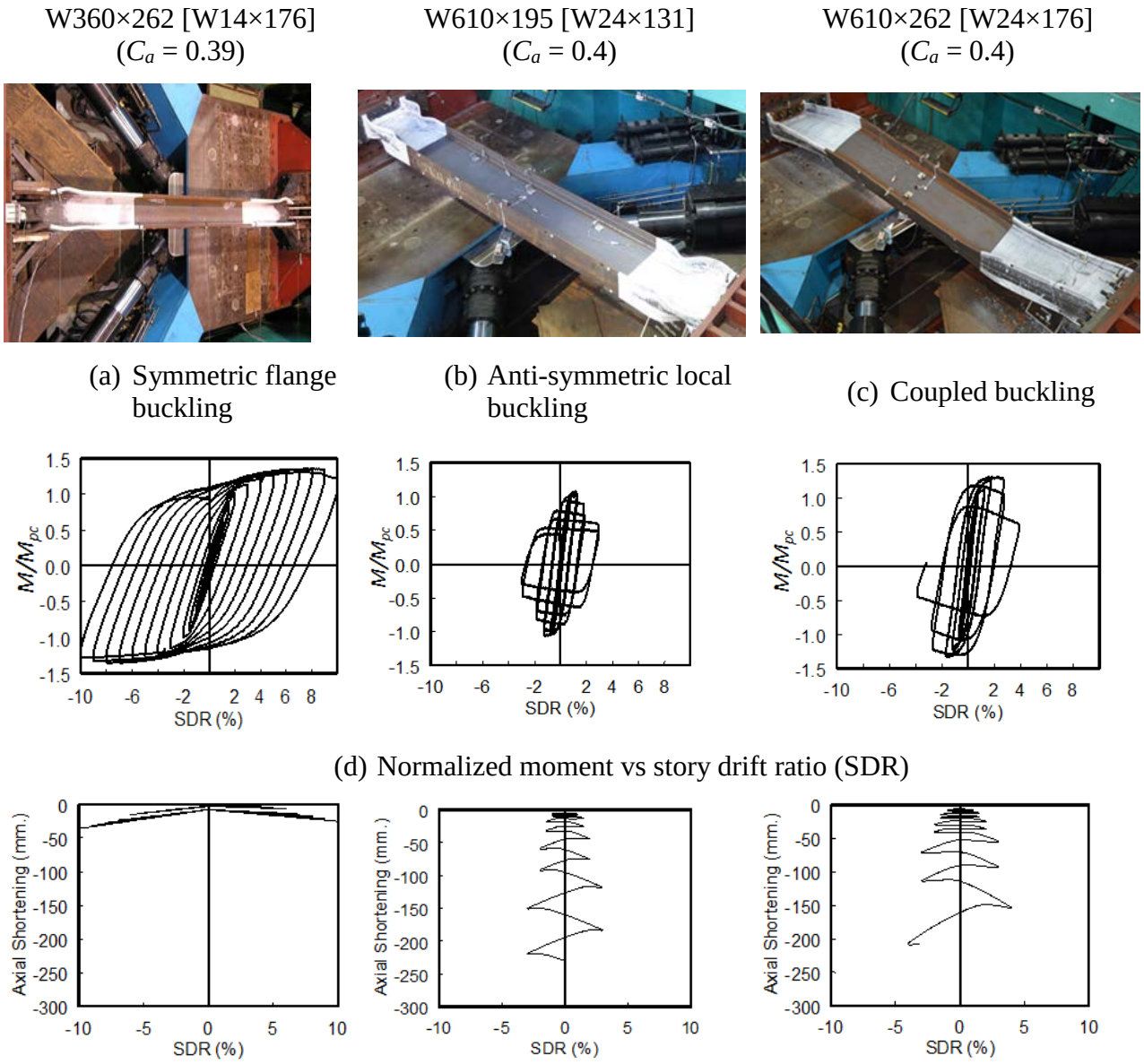

(a) Symmetric flange buckling

(b) Anti-symmetric local buckling

(c) Coupled buckling

(d) Normalized moment vs story drift ratio (SDR)

(e) Axial shortening vs story drift ratio (SDR)

Fig. 1 Column cyclic behaviour and axial shortening of different failure modes

(a) SFB

(b) ALB

Fig. 2 Symmetric flange buckling and antisymmetric local buckling

As shown in Fig. 2 local buckling in the plastic hinges develop a symmetric flange buckling (SFB). However, the deeper W610 [W24] column reached a much lower story drift than the W360 [W14]. Plastic hinging in the W610 [W24] column resulted in significant strength degradation from local buckling [Fig. 1(b)] or a combination of local buckling and LTB [Fig. 1(c)] and column shortening. Contrary to the W360 [W14], Fig. 2(b) shows an anti-symmetric local buckling (ALB) pattern when plastic hinging with local buckling occurs in the plane of bending. Fig. 1(c) depicts a third buckling pattern–coupled buckling (CB)–when local buckling within the plastic hinge interacts with LTB.

For modelling purposes, it is desirable to have a simple procedure to identify the governing buckling mode for cyclically-loaded wide-flange columns. Ozkula et al. [9] recently proposed a procedure for this purpose. The buckling mode is governed by the parameter ζ [10]:

$$\zeta = \xi \left(\frac{t_f}{t_w}\right)^2 \tag{3}$$

where

$$\xi = \frac{2}{C_s}\frac{\lambda_w}{\lambda_f} \tag{4}$$

and C_s is a non-dimensional web stiffness factor:

$$C_s = \frac{2\pi c \sinh^2 \pi c}{(\sinh \pi c \cosh \pi c - \pi c)} \tag{5}$$

The coefficient c in the above equation is the effective aspect ratio of the web:

$$c = \frac{2h/b_f}{3.93\left(\frac{t_w}{t_f}\right) + 3.54} \tag{6}$$

where h is the distance between flanges (= $d - t_f$). Fig. 3 shows the value for ζ for each test specimen. The figure also shows that values of ζ equal to 4.25 and 8 can be used to separate the three buckling modes discussed previously.

Although steel moment frames are usually designed using an elastic analysis procedure, they are expected to experience significant inelastic deformations under large earthquakes. For performance-based design or assessment, nonlinear analysis is sometimes required to evaluate the behaviour of the structure. In the U.S., ASCE/SEI 41-13 [7] is commonly used for this purpose. Unfortunately, little guidance is available concerning the inelastic modelling of columns subjected to combined axial and flexural loading.

For use in nonlinear evaluation of steel moment frames, the objective of this paper is to propose a cyclic backbone curve for a wide-flange steel column that considers the type of governing buckling mode. Since the available test database on the cyclic behaviour of full-scale columns is limited, finite element simulations of more than one hundred columns was conducted and the results used for a multivariate regression analysis for developing these backbone curves.

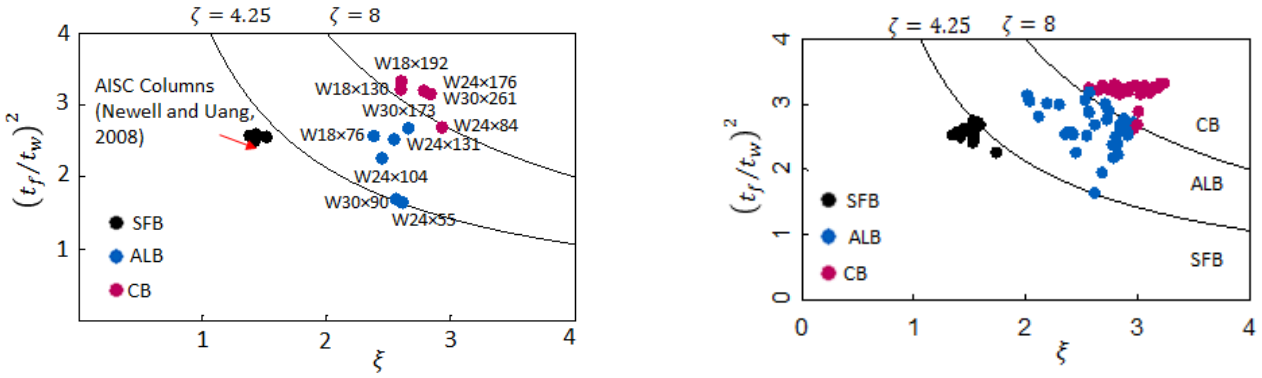

(a) Experimental results (b) Numerical analysis results

Fig. 3 Validation of proposed criterion with experimental and simulation results

2 FINITE ELEMENT MODELLING VALIDATION AND PARAMETRIC STUDY

Finite element (FE) models of the NIST test specimens were created and analyzed using ABAQUS [11]. Based on the test results of the W24 columns, a correlation study was first conducted to validate the modelling technique. Sample correlation of two test specimens (Specimen 1L with a W610×262 [W24×176] section and Specimen 3L with a W610×155 [W24×104] section, both with C_a = 0.2) is presented in Fig. 4. The figure shows that the buckling mode and global response, including axial shortening, of the tested columns were adequately simulated by the FE analysis.

One hundred and ten wide-flange columns with sections found in Part 1 of the AISC Manual of Steel Construction [12] were analyzed through FE analysis. These sections ranged from W1100 [W44] to W250 [W10] sections and covered a wide range of slenderness parameters [13]:

$$2.62 \le \lambda_f \le 10.2; \quad 5.66 \le \lambda_w \le 54.6; \quad 41.1 \le \lambda_L \le 88.89 \tag{7}$$

Fig. 5 shows the distribution of the flange and web width-to-thickness ratios. The limiting width-thickness ratios for highly ductile (λ_{hd}) and moderately ductile (λ_{md}) sections prescribed in AISC 341 are also shown in the figure. Based on the procedure proposed by Ozkula et al. [9], and described in Section 1, the predicted governing buckling mode of each simulated column is indicated in the figure.

For analysis, each column was cyclically loaded with the AISC loading protocol with three levels of constant axial compressive force (C_a = 0.2, 0.4, and 0.6). The yield stress, F_y, was 379 MPa [55 ksi]. To evaluate the effect of variations of material yield stress, two additional yield stress levels, 345 and 448 MPa [50 and 65 ksi], were analysed, but for C_a = 0.2 only. Therefore, the numerical database included a total of 1,100 cases. Fig. 6 shows the response of three columns. As expected, the stocky W310 [W12] column produces a very stable hysteretic response, while the deeper, slenderer W460 [W18] and W920 [W36] columns) experienced a rapid strength and stiffness degradation. The observed buckling mode for each simulated column was also compared with the predicted mode. The comparison in Fig. 3(b) shows that the procedure proposed by Ozkula et al. [9] appears reliable.

3 CONSTRUCTION OF CYCLIC BACKBONE CURVES

3.1 ASCE 41 Backbone Curves

Nonlinear response of steel moment frames from an earthquake excitation can be analyzed by using the concentrated hinge model, the distributed hinge model, or the continuum finite element model [14]. The concentrated hinge model is commonly used in practice due to its simplicity and efficiency. For this purpose, ASCE 41 specifies cyclic backbone curves like that shown in Fig. 7(a) to model the actions (e.g., flexure) in structural components.

W610×262 [W24×176] (C_a = 0.2) W610×155 [W24×104] (C_a = 0.2)

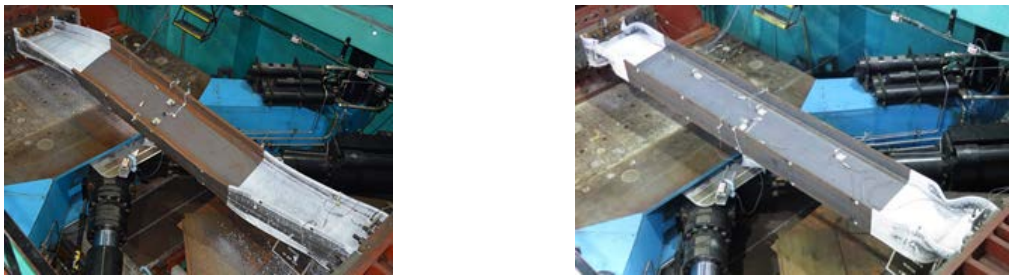

(a) from tests

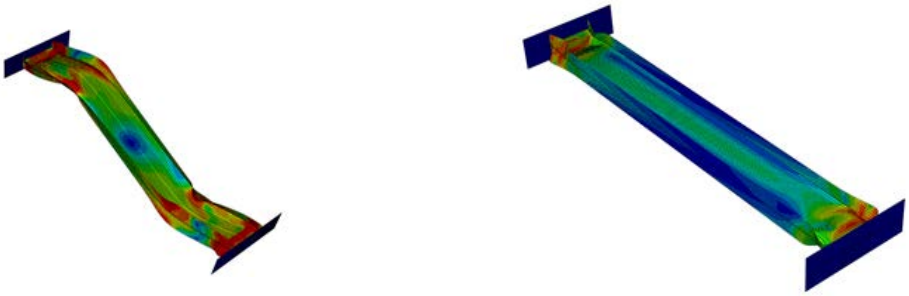

(b) from FE simulation

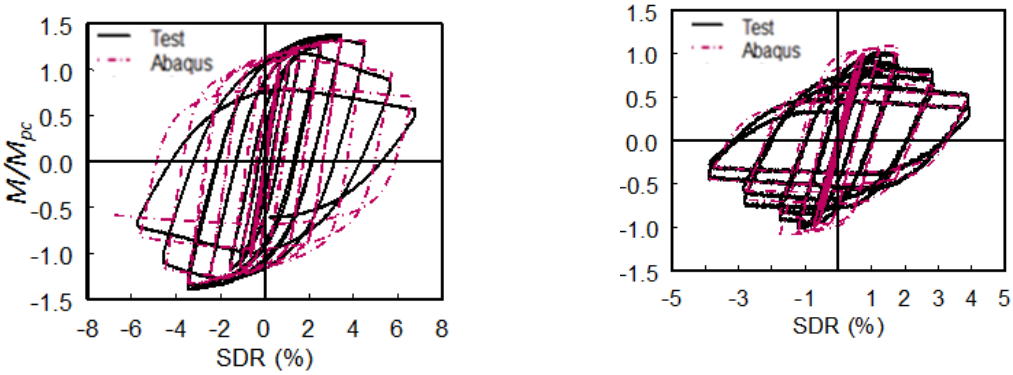

(c) Cyclic response

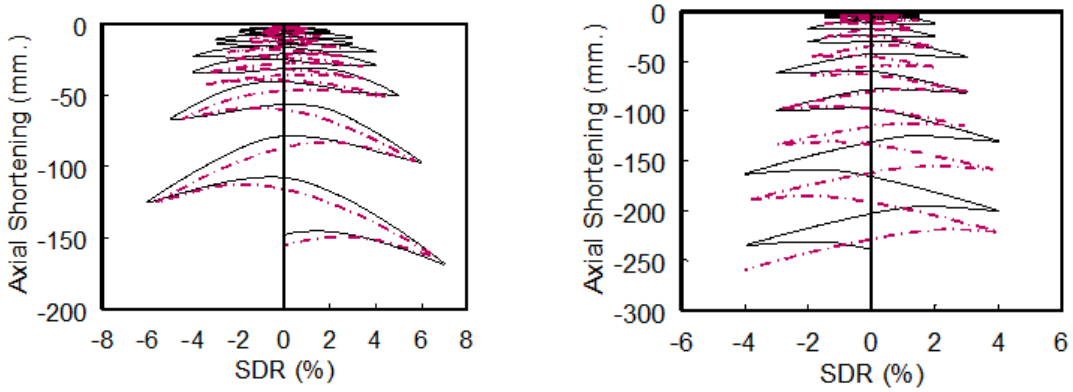

(d) Axial shortening

Fig. 4 Correlation of column test results and finite element simulation (continued)

The generalized backbone curve is composed of four zones. Zone 1 represents the elastic response. Zones 2 and 3 define the pre- and post-buckling region, respectively. Zone 4 represents the residual strength (if any) of the structural component. While it is reasonable to assume a residual strength zone for beams, with the presence of axial compression, however, the NIST column test program showed that columns tended to lose complete flexural strength and did not exhibit the plateau-like residual strength.

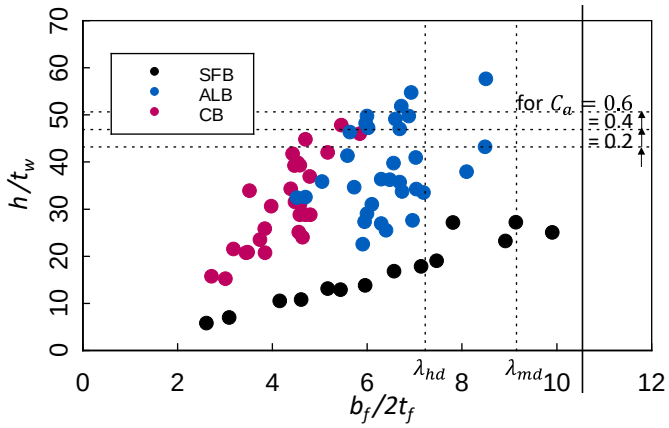

Fig. 5 Distribution of width-to-thickness ratios of selected sections

Therefore, the column cyclic backbone curve proposed herein has only three zones as shown in Fig. 7(b). The backbone curve is affected by the loading history [14]. Fig. 7(b) shows three curves representing those produced by the symmetric AISC cyclic loading protocol, a near-fault loading protocol, and a monotonic loading protocol, respectively. The curve produced by the AISC loading protocol is potentially conservative, while the curve produced by the monotonic loading is potentially overly unconservative for predicting the seismic response. The actual response in an earthquake is likely to be bounded by these two curves. In the following, backbone curves correspond to those produced by the AISC symmetric loading protocol and monotonic loading are established.

3.2 Regression Analysis

3.2.1 Analysis Procedure

To construct the backbone curves, several response variables (RVs) on the curve were established from nonlinear multivariate regression analysis. To determine an appropriate functional form, flange and web local slenderness parameters (b_f / $2t_f$, (λ_f) and h / t_w, (λ_w), respectively) were considered. In addition, some parameters like (L / r_y), h / b_f, L / d , t_f / t_w, and λ_w / λ_f were also included.

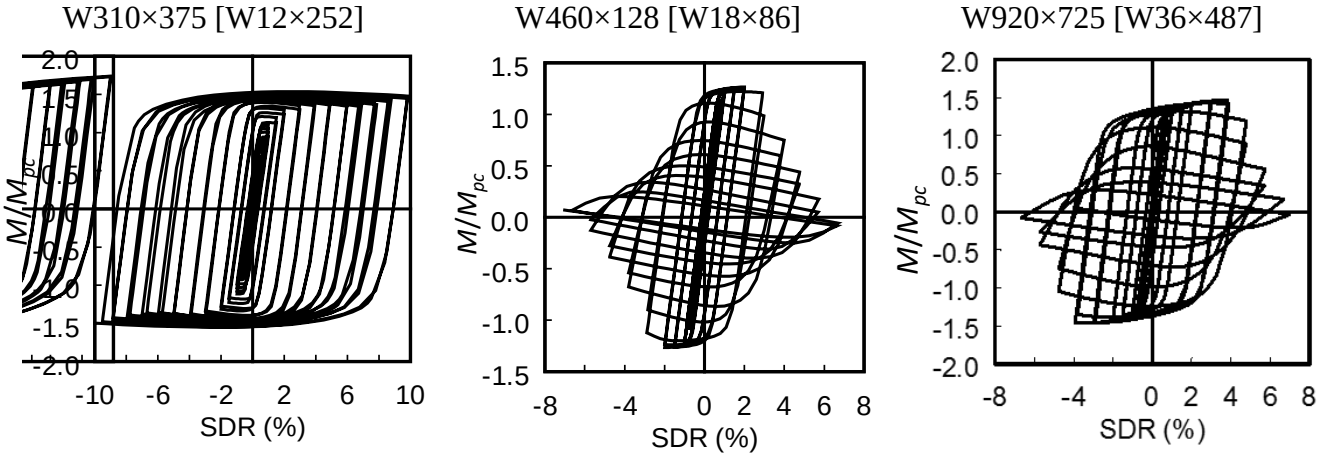

(a) Global response

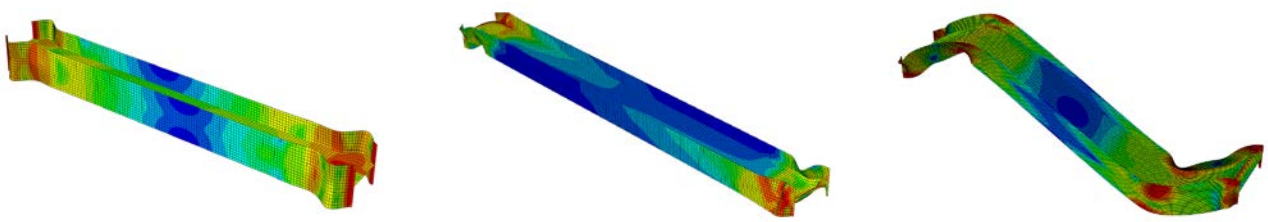

(b) Failure mode

Fig. 6 Sample cyclic response and failure mode of numerical models

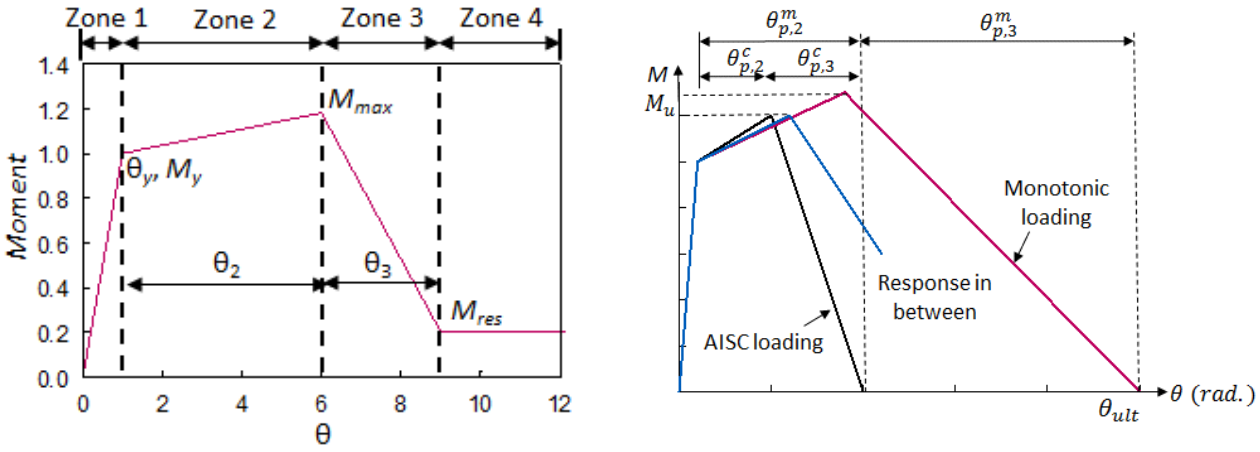

(a) ASCE 41 backbone curve (b) Proposed backbone curve

Fig. 7 Cyclic backbone curves

Sensitivity analyses were performed to find the statistical importance of each parameter. Using the stepwise multivariate regression analysis approach, only the variables that were statistically important were included in the predictive equation. The following general nonlinear model was used:

$$RV = a_1 \lambda_f^{a_2} \lambda_w^{a_3} \lambda_L^{a_4} \left(1 - \frac{P_u}{P_y}\right)^{a_5} \tag{8}$$

where coefficients a_1 are a_5 constants to be determined from regression, P_u= applied axial force, and other terms have been defined.

Other than considering the entire database from the parametric study for regression analysis, the database was subdivided into three groups based on the governing buckling mode (SFL, ALB, or CB) defined earlier. It is believed that performing a regression analysis for each buckling mode will not only reduce the scatter but also produce a more accurate prediction of the backbone curve.

3.2.2 Zone 1

The elastic flexural stiffness, K_e, full-yield flexural strength, M_y, and elastic yield rotation, θ_y, are defined as follows:

Elastic flexural stiffness, K_e:

$$K_e = \frac{6EI_x}{L}\left(1 - \frac{P_u}{P_e}\right) \tag{9a}$$

where

$$P_e = \frac{\pi^2 EI_x}{L^2} \tag{9b}$$

Yield flexural strength, M_y: Based on Equations H1-1a and H1-1b in AISC 360 [15], M_y is computed as follows: M_y=M_{pc} and
when $P_u/P_y \geq 0.2$

$$M_y = \frac{9}{8} M_p \left(1 - \frac{P_u}{P_y}\right) \tag{10}$$

when $P_u/P_y < 0.2$

$$M_y = M_p \left(1 - \frac{P_u}{2P_y}\right) \tag{11}$$

Chord rotation at full yield, θ_y:

$$\theta_y = M_{pc}/K_e \tag{12}$$

3.2.3 Zones 2 and 3

Pre-buckling plastic rotation, θ_{p2}, and maximum moment, M_{max}, are needed to define Zone 2. The maximum moment can also be normalized by M_y and is defined as the strain hardening ratio, α. Zone 3 is defined by the post-buckling rotation, θ_{p3}.

(a) SFB Mode

For the monotonic curve, regression yields the following results, where R^2 is the coefficient of determination:

$$\alpha^m = 10^{0.44}\lambda_f{}^{-0.33}\left(1-\frac{P}{P_y}\right)^{-0.60} \quad (R^2=0.96) \quad (13a)$$

$$\theta_{p2}^m = 10^{-1.93}\lambda_f{}^{-1.44}\left(1-\frac{P}{P_y}\right)^{0.85}\left(F_y\right)^{1.37} \quad (R^2=0.91) \quad (13b)$$

$$\theta_{p3}^m = 10^{-0.48}\lambda_f{}^{-0.47}\left(1-\frac{P}{P_y}\right)^{1.57}\left(F_y\right)^{0.29} \quad (R^2=0.90) \quad (13c)$$

For the cyclic backbone curve, the parameters are given as follows:

$$\alpha^c = 10^{0.44}\lambda_f{}^{-0.49}\left(1-\frac{P}{P_y}\right)^{-0.36} \quad (R^2=0.88) \quad (14a)$$

$$\theta_{p2}^c = 10^{-3.0}\lambda_f{}^{-1.8}\left(1-\frac{P}{P_y}\right)^{1.5}\left(F_y\right)^{2.0} \quad (R^2=0.91) \quad (14b)$$

$$\theta_{p3}^c = 10^{-3.98}\lambda_f{}^{-0.79}\left(1-\frac{P}{P_y}\right)^{1.94}\left(F_y\right)^{2.08} \quad (R^2=0.90) \quad (14c)$$

Regression analysis conducted by Newell and Uang [6] showed that λ_w has a strong influence on the cyclic response of W14 columns, whose response was governed by SFB, and L / r_y has a weak influence. Note that λ_f, not λ_w, appears in the above equations. This is because there is a strong correlation between λ_f and λ_w for the shallow sections listed in the AISC Steel Construction Manual and one of the terms is automatically dropped out in regression. Since flange local buckling is dominant when SFB occurs, it is more logical to keep λ_f instead of λ_w in the expressions.

(b) ALB Mode

It is expected that both λ_f and λ_w play an important role on the response when ALB occurs. The regression results do support this expectation. For the monotonic curve:

$$\alpha^m = 10^{0.66}\lambda_f{}^{-0.20}\lambda_w{}^{-0.22}\left(1-\frac{P}{P_y}\right)^{-0.60} \quad (R^2=0.90) \quad (15a)$$

$$\theta_{p2}^m = 10^{2.78}\lambda_f{}^{-0.31}\lambda_w{}^{-1.91}\left(1-\frac{P}{P_y}\right)^{1.40}\left(F_y\right)^{-0.3} \quad (R^2=0.85) \quad (15b)$$

$$\theta_{p3}^m = 10^{2.42}\lambda_f{}^{-0.21}\lambda_w{}^{-0.1}\left(1-\frac{P}{P_y}\right)^{2.10}\left(F_y\right)^{-1.45} \quad (R^2=0.80) \quad (15c)$$

For the cyclic backbone curve:

$$\alpha^c = 10^{0.34}\lambda_f{}^{-0.2}\lambda_w{}^{-0.1}\left(1-\frac{P}{P_y}\right)^{-0.36} \quad (R^2=0.91) \quad (16a)$$

$$\theta_{p2}^c = 10^{0.1}\lambda_f{}^{-0.5}\lambda_w{}^{-1.9}\left(1-\frac{P}{P_y}\right)^{2.5}\left(F_y\right)^{0.9} \quad (R^2=0.85) \quad (16b)$$

$$\theta_{p3}^c = 10^{1.1}\lambda_f{}^{-0.47}\lambda_w{}^{-2.2}\left(1-\frac{P}{P_y}\right)^{2.74}\left(F_y\right)^{0.9} \quad (R^2=0.90) \quad (16c)$$

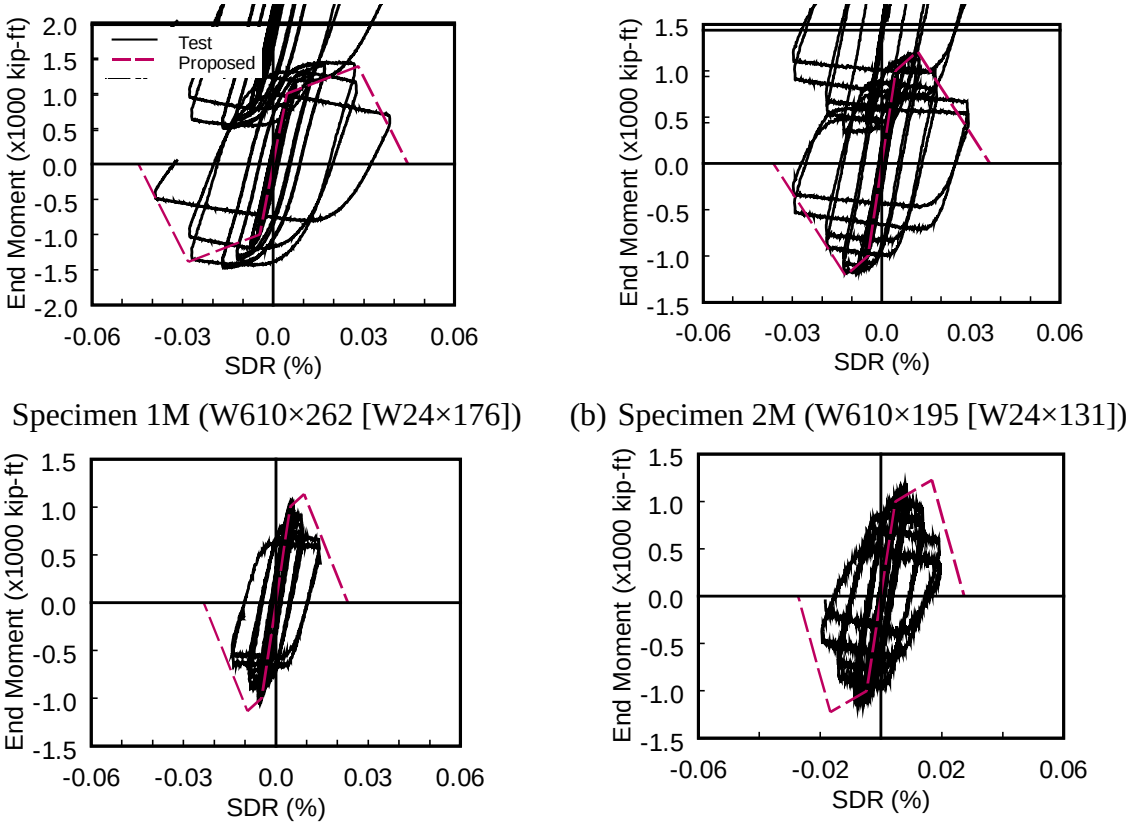

(a) Specimen 1M (W610×262 [W24×176]) (b) Specimen 2M (W610×195 [W24×131])

(c) Specimen 3M (W610×155 [W24×104]) (d) Specimen 4M (W610×125 [W24×84])

Fig. 8 Comparison of experimental response with proposed cyclic backbone curves

(c) CB Mode:

Experimental testing and numerical simulation showed that CB mode would not occur under monotonic loading because a steel column cannot strain harden enough to increase the yielded length in the hinging region to trigger LTB. In this case, Eq. (15) can be used; this equation was obtained in regression by combining the data from columns experiencing either ALB or CB. For the cyclic backbone curve:

$$\alpha^c = 10^{0.55}\left(\frac{\lambda_w}{\lambda_f}\right)^{-0.13}\lambda_L{}^{-0.2}\left(1-\frac{P}{P_y}\right)^{-0.36} \qquad (R^2=0.86) \qquad (17a)$$

$$\theta_{p2}^c = 10^{1.7}\left(\frac{\lambda_w}{\lambda_f}\right)^{-2.1}\lambda_L{}^{-0.3}\left(1-\frac{P}{P_y}\right)^{2.8}\left(F_y\right)^{-0.38} \qquad (R^2=0.93) \qquad (17b)$$

$$\theta_{p3}^c = 10^{1.18}\left(\frac{\lambda_w}{\lambda_f}\right)^{-0.67}\lambda_L{}^{-0.65}\left(1-\frac{P}{P_y}\right)^{3.35}\left(F_y\right)^{-0.38} \qquad (R^2=0.86) \qquad (17c)$$

Fig. 8 shows the comparison of proposed backbone curves using the equations above and the test results. Backbone curves predicted the bounds of the hysteresis loops well.

4 CONCLUSIONS

For seismic design, wide-flange columns in steel moment frames are expected to form plastic hinges at the column bases. When shallow, stocky sections are used, symmetric flange buckling would occur during the hinging process. Recently, engineers prefer to use deeper, slenderer sections to meet stringent story drift requirements. Deep columns, however, have larger slenderness ratios for local and global buckling control than shallow columns. Testing showed that either severe flange and web local buckling or local buckling in combination with lateral-torsional buckling would become the dominant failure mode of deep, slender columns. This failure mode is accompanied by a significant degradation in strength and stiffness. Therefore, cyclic backbone curves that consider local

and global slenderness and the governing buckling mode are needed for performance-based evaluation of the nonlinear response of steel moment frames.

Finite element simulation of 110 steel columns that cover a wide range of slenderness ratios, axial force level, and yield stress level was conducted to generate a database for regression analysis; both cyclic and monotonic analyses were conducted. A correlation study with full-scale test results of steel columns was conducted to validate the numerical procedure. The cyclic buckling modes of the simulated columns were found to correlate well with those predicted by the procedure proposed by Ozkula et al. [9]. Expressions that define the key parameters for the monotonic and cyclic backbone curves for symmetric flange buckling, anti-symmetric local buckling, and coupled buckling were presented.

DISCLAIMER

Certain commercial software, equipment, instruments, or materials may have been used in the preparation of information contributing to this paper. Identification in this paper is not intended to imply recommendation or endorsement by NIST, nor is it intended to imply that such software, equipment, instruments, or materials are necessarily the best available for the purpose.

No formal investigation to evaluate potential sources of uncertainty or error, or whether multiple sources of error are correlated, was included in this study. The question of uncertainties in the analytical models, solution algorithms, material properties and component dimensions and positions employed in tests and analyses are beyond the scope of the work reported here.

REFERENCES

[1] AISC (2010). *Seismic Provisions for Structural Steel Buildings*. ANSI/AISC 341-10, American Institute of Steel Construction, Chicago, IL.
[2] AISC (2010). *Prequalified Connections for Special and Intermediate Steel Moment Frames for Seismic Applications*. ANSI/AISC 358-10, American Institute of Steel Construction, Chicago, IL.
[3] ASCE (2010). *Minimum Design Loads for Buildings and Other Structures*, ASCE 7, American Society of Civil Engineering, Reston, VA.
[4] Fogarty, J., and El-Tawil, S. (2016). "Collapse Resistance of Steel Columns under Combined Axial and Lateral Loading", *Journal of Structural Engineering*, Vol. 142, No. 1, ASCE.
[5] Ozkula, G., Harris, J., and Uang, C.-M. (2017). "Observations from Cyclic Tests on Deep, Wide-Flange Beam-Columns", *Engineering Journal*, 1st Quarter, AISC, pp. 45-59.
[6] Newell, J.D. and Uang, C.-M. (2008). "Cyclic Behaviour of Steel Wide-Flange Columns Subjected to Large Drift," *Journal of Structural Engineering*, Vol. 134, No. 8, pp. 1334-1342, ASCE.
[7] ASCE (2013). *Seismic Rehabilitation of Existing Buildings*, ASCE 41, American Society of Civil Engineers, Reston, VA.
[8] NEHRP. (2011). "Research Plan for the Study of Seismic Behaviour and Design of Deep, Slender Wide Flange Structural Steel Beam-Column Members," *NIST-GCR-11-917-13*, Gaithersburg, MD.
[9] Ozkula, G., Harris, J., and Uang, C.-M. (2017). "Classifying Cyclic Buckling Modes of Steel Wide-Flange Columns under Cyclic Loading," *Structures Congress*, pp. 155-167, ASCE/SEI, Denver, Colorado.
[10] Han, K.-H., and Lee, C.-H. (2016). "Elastic Flange Local Buckling of I-Shaped Beams Considering Effect of Web Restraint," *Thin-walled Structures*, Vol. 105, pp. 101-111, Elsevier.
[11] ABAQUS-FEA/CAE. (2011). Dassault Systemes Simulia Corp., RI.
[12] AISC (2010). *Steel Construction Manual*. American Institute of Steel Construction, Chicago, IL.
[13] Ozkula, G., and Uang, C.-M. (2015). "Seismic Behaviour and Design of Deep, Slender Wide-Flange Structural Steel Beam-Column Members," *Rep. No. SSRP-15/06*, Department of Structural Engineering, University of California, San Diego, La Jolla, CA.
[14] NEHRP. (2017). "Guidelines for Nonlinear Structural Analysis for Design of Buildings: Part II-a Steel Moment Frames," *NIST-GCR-11-917-13*, Gaithersburg, MD.
[15] AISC (2010). *Specification for Structural Steel Buildings*. ANSI/AISC 360-10, American Institute of Steel Construction, Chicago, IL.